

Combustion of Model Compositions Based on Furazanotetrazine Dioxide and Dinitrodiazapentane. I. Binary Systems

V. N. Simonenko^a, P. I. Kalmykov^b, A. B. Kiskin^a,
O. G. Glotov^a, V. E. Zarko^a, K. A. Sidorov^b,
B. V. Pevchenko^b, and R. G. Nikitin^b

UDC 536.46

Published in *Fizika Goreniya i Vzryva*, Vol. 50, No. 3, pp. 68–77, May–June, 2014.
Original article submitted April 5, 2013.

Abstract: The combustion behavior of high-energy systems based on furazano[3,4-e]tetrazine-4,6-dioxide and 2,4-dinitro-2,4-diazapentane with metal and energetic additives (Al, AlH₃ ammonium perchlorate, ammonium dinitramide, and HMX) has been studied. The burning rate, combustion stability, and characteristic combustion temperatures with pressure variation are estimated. It is found that there is a critical burning rate above which a deflagration-to-explosion transition occurs. The critical conditions depend on the formulation of the compositions.

Keywords: furazano[3,4-e]tetrazine-4,6-dioxide (furazanotetrazine dioxide, FTDO), 2,4-dinitro-2,4-diazapentane (DNP), eutectics, [1FTDO–1DNP] molecular compound, burning rate, deflagration-to-explosion transition, combustion-wave temperature.

DOI: 10.1134/S0010508214030083

INTRODUCTION

The current level of development of special equipment and technologies is characterized by the use of individual powerful explosives, such as RDX, HMX, ammonium dinitramide (ADN), hexanitrohexaazaisowurtzitane (HNIW), etc., in compositions of energetic condensed systems [1–5]. This is dictated by the need to increase the energy and other characteristics of tested compositions under development. In parallel with studies of existing substances, efforts are directed toward the development of new energetic compounds. One of these is furazanotetrazine dioxide (FTDO) [6, 7]—a compound of the series polynitrogen diazene oxides with a high enthalpy of formation ($\Delta H_f^0 \geq 4300$ kJ/kg) [8, 9]. This value of ΔH_f^0 deter-

mines the interest in FTDO as a candidate for use in high-energy compositions.

Energetic compounds exhibit considerable sensitivity to mechanical stress [9, 10], high burning rate, and typical combustion instability at elevated pressure—transition to explosion. Safe use of FTDO is possible when it is used jointly with less sensitive compounds, such as low-melting nitramines or nitrotriazoles [11].

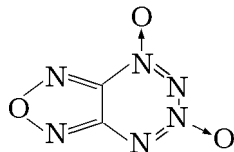
This paper presents data on the properties and combustion behavior of FTDO as well as the results of experimental studies of combustion of mixtures based on FTDO and 2,4-dinitro-2,4-diazapentane (DNP), a linear nitramine. The objective of the study was to evaluate the effect of formulation factors (primarily the FTDO/DNP ratio and the presence of various types of additives) on the burning rate and combustion behavior of compositions at elevated pressure p . Also, the thermal parameters of combustion wave are evaluated using the results of thermocouple measurements at atmospheric pressure (with photo and video recording) and at elevated pressure.

^aVoevodsky Institute of Chemical Kinetics and Combustion, Siberian Branch, Russian Academy of Science, Novosibirsk, 630090 Russia; sim@kinetics.nsc.ru; glotov@kinetics.nsc.ru.

^bAltai Federal Research and Production Center, Biisk, 659322 Russia.

**PROPERTIES OF FTDO
AND POSSIBILITY OF REDUCING
THE SENSITIVITY OF SYSTEMS
BASED ON IT**

The new promising high-energy compound FTDO of the general formula $C_2N_6O_3$

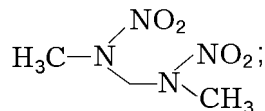


is superior in a number of parameters to traditional energetic materials and is therefore attracting increased interest at present.

The unique combination of two conjugate diaza-N-oxide groups annulated into the tetrazine dioxide cycle of 1,2,3,4-tetrazine-1,3-dioxide, combined with the other energetic heterocycle (furazane), provides stability of the FTDO molecule. The substance has a high density (1.84 g/cm^3), high content of oxygen (30.75%) and nitrogen (53.85%), and a considerable enthalpy of formation (according to different estimates, $\Delta H_f^0 \geq 4300 \text{ kJ/kg}$). Table 1 shows the physicochemical and energy characteristics of FTDO in comparison with known cyclic and caged nitramines. The properties listed above make energetic condensed systems based on FTDO promising materials [12].

It is seen from Table 1 that, along with increased energy parameters, FTDO is characterized by high impact sensitivity, high burning and detonation velocities, high calculated combustion temperature, and low critical detonation thickness. The friction sensitivity of FTDO is at the level of sensitivity of HNIW.

To ensure safe use of FTDO, having analyzed experimental and literature data [11, 16–21], we selected and tested an approach based on dilution of FTDO with a less sensitive component. 2,4-dinitro-2,4-diazapentane (DNP) was used as such component. Its main characteristics are as follows: general formula $C_3H_8N_4O_4$,



$T_m = 55^\circ\text{C}$, $\Delta H_f^0 = -132.3 \text{ kJ/kg}$, $\rho = 1.51 \text{ g/cm}^3$, $T_f = 2116 \text{ K}$ (at $p = 7 \text{ MPa}$), and $u = 0.85, 4.0$, and 8.1 mm/s at $p = 2, 10$, and 20 MPa , respectively; the exponent in the pressure dependence of the burning rate $n = 1.04$ at $p = 2\text{--}20 \text{ MPa}$ [22].

The choice of DNP is due to its energy content, heat resistance, chemical compatibility with FTDO, comparative safety in handling, and accessibility for

use in energetic compositions for different applications. DNP has good thermodynamic affinity to FTDO, and their co-crystallization from the melt at a ratio FTDO/DNP = 49/51 yields a congruently melting and partially dissociated solid molecular compound (hereinafter, referred to as MC) of equimolecular composition [1FTDO–1DNP] [11, 16–21]. At certain ratios of FTDO/DNP, the system has eutectics, some of whose properties will be discussed below.

Reduction in the thermal and mechanical sensitivity of the FTDO/DNP mixture compared with that of pure FTDO has been confirmed experimentally. In addition, MC has lower sensitivity than the mechanical mixture of the same composition (Table 2).

Crystalline FTDO samples of bulk density ignite and burn in air to produce a bright blue-violet flame. Their burning is accompanied by an explosive reaction with a typical blast sound.

Data on the burning rate of FTDO as an individual substance are scarce. In [13], burning rates were determined for FTDO samples in the form of plates 1.5–2 mm wide, 10 mm long, and 0.5–0.7 mm thick, pressed at a pressure 500–600 MPa to a density of $1.70\text{--}1.73 \text{ g/cm}^3$ (92–94% of the maximum). The samples were immersed in liquid halogenated oil which acted as an inhibitor. In the range $p = 0.1\text{--}10 \text{ MPa}$, the burning rate is described by the equation $u = 18.9p^{0.7} \text{ [mm/s]}$ ($u \approx 4 \text{ mm/s}$ at $p = 0.1 \text{ MPa}$ and $u \approx 100 \text{ mm/s}$ at $p = 10 \text{ MPa}$). In our opinion, these data need to be confirmed. In particular, it is necessary to elucidate the effects of the type of inhibitor material and the characteristic dimensions of the sample on the burning rate.

We investigated combustion of crystalline FTDO in a constant-volume manometric bomb using the method of investigating transition processes [23–25] at increasing pressure. The experiments were carried out with samples of 10 mm high and 10 mm in diameter, composed of $\varnothing 10 \times 1 \text{ mm}$ pellets compacted to a density of $1.50\text{--}1.55 \text{ g/cm}^3$ (81–84% of the maximum density of FTDO). The pellets were tightly inserted into a fluoroplastic cup and slightly packed. The sample had minimum porosity and was actually shielded on the lateral surface and on the bottom. The volume of the bomb was $V = 120 \text{ cm}^3$, the initial pressure was 0.1 MPa, and the final pressure 98 MPa. The time of combustion of the sample under these conditions was 5–6 ms, which probably indicates a convective burning regime.

At a pressure close to atmospheric pressure, solidified¹ FTDO–DNP mixtures burn steadily, but at elevated pressures, their deflagration can transform to

¹Instead of the term crystallization we deliberately use the more general concept of solidification to denote the change in the state of the system from liquid to solid.

Table 1. Main characteristics of energetic compounds [1, 4, 5, 8–15]

Characteristics	Values of characteristics			
	RDX	HMX	HNIW	FTDO
Density ρ , g/cm ³	1.82	1.90	2.04	1.84
Oxidizer excess ratio	0.67	0.67	0.80	0.75
Enthalpy of formation ΔH_f , kJ/kg	320	296	950	4321
Melting point T_m , °C	205 with decomposition	280 with decomposition	—	112–114
Temperature at the beginning of intense decomposition, °C	>205	>280	228–264	134–140
Lower impact sensitivity limit (device No. 2, weight 10 kg)	75	70	50	30–70
Lower friction sensitivity limit, kg · s/cm ² (device K-44-III)	2200	2100	1200	900–1500
Burning rate u , mm/s (at 10 MPa)	17.8	19.0	31.5	100
Exponent n in the power burning law $u = Bp^n$ (at $p = 0.1$ – 10 MPa)	0.82	0.89	0.74	0.7
Calculated adiabatic combustion temperature T_f , K (at $p = 10$ MPa)	3320	3295	3635	4516
Detonation velocity, m/s (ρ in g/cm ³)	8750 (1.80)	9100 (1.90)	9500 (1.85)	5500 (0.60) 7000 (0.80) 9600 (1.55)
Critical detonation diameter, mm	0.6–1.0	0.5–1.0	0.2–0.5	0.02–0.04

an explosion. This phenomenon will be considered in more detail when discussing the results of studying the FTDO–DNP based systems. Obviously, partial replacement for FTDO by DNP reduces the potential energy content of the system. At the same time, the energy content of FTDO is so high (see Table 1) that even with the replacement of half, FTDO is superior in energy to conventional formulations. There is evidence [26] of a relatively high sensitivity of the eutectic mixture FTDO/DNP = 65/35 to a laser pulse. When the CO₂ laser radiation density exceeds a certain threshold value, an explosive transformation occurs. The threshold level is 18–21 J/cm² for different solidification conditions of the melt of the mixture.

SAMPLES AND EXPERIMENTAL TECHNIQUE

To estimate the pressure dependence of the burning rate $u(p)$, we used a high-pressure reaction vessel of 2 liters with nitrogen in which samples weighing up to 1.5 g were burned at a pressure of 2–8 MPa. The design

of the vessel allows simultaneous placement of 12 samples with dimensions $d = 7$ – 10 mm, and $h = 10$ mm, which can be ignited individually. Samples were prepared by pouring a molten mass in ebony cups, followed by solidification in a given mode. Each sample was ignited over the entire surface of the open end by a flame torch generated by an igniting composition attached to a Nichrome wire heated by electric current. The wire was placed at a distance of ≈ 1 mm above the sample surface. A standard manometer and an LKh-412 pressure gauge were used for pressure monitoring. The burning rate was calculated by dividing the sample length by the combustion time determined from the recorded curve of $p(t)$. The pressure rise depends on the size of the sample, its burning rate, and initial pressure. The typical pressure rise was ≈ 0.4 MPa at $p = 4$ MPa. The average pressure in the experiment was calculated as the arithmetic mean of the initial and final values. The data were fitted by a power law $u(p) = Bp^n$.

For additional control of the combustion stability, we recorded the signal from a microphone mounted on the outer wall of the vessel. As a rule, a failure of stable combustion (deflagration-to-explosion transition) is ac-

Table 2. Comparison of pure FTDO and FTDO–DNP systems in the ratio of 1 : 1

Characteristics	Values of characteristics		
	FTDO	FTDO/DNP = 50/50	[1FTDO–1DNP]
Melting point T_m [°C]	112–114	51	62
Temperature at the beginning of intense decomposition [°C]	134–140	137–150	162–165
Thermal stability in vacuum characterized by gasification (ampoule-chromatographic method) at 50°C for 24 h, V [cm ³ /100 mg]	0.018	0.012	0.009
Impact sensitivity (device No. 2, weight 2 kg), lower limit [mm]	30–50	70–100	150–200
Friction sensitivity (device K-44-III), lower limit [kg · s/cm ²]	1200–1500	1500	1600
Critical detonation diameter [mm]	0.02–0.04	0.62	0.70
Maximum density [g/cm ³]	1.84	1.61	1.71

accompanied by characteristic clip-clopping sound, which is detected by the microphone as an impact type signal.

Information on the characteristic temperatures in the combustion wave was obtained by thermocouple measurements. A description of the measurements (type, shape, and embedding of thermocouples, signal processing, etc.) is given below.

RESULTS OF EXPERIMENTS WITH THE BINARY COMPOSITIONS

Previously [11, 16–21], phase equilibria in the FTDO–DNP system have been studied using differential thermal analysis (DTA), differential scanning calorimetry (DSC), and microcalorimetry, and a melting diagram was constructed.

The x – T phase diagram has two eutectics (E_1 and E_2), and the molecular compound (MC) is located between them. The melting points T_m and component ratios for MC, E_1 , and E_2 are presented in Table 3. In the first phase of research, we studied binary compositions with variation of the FTDO/DNP ratio. Four ratios were selected that roughly corresponded to the E_1 and E_2 eutectics, MC, and an intermediate composition between MC and E_2 . Then, a metal (ASD-6 aluminum or aluminum hydride AlH_3 in an amount of 2.5, 3, or 5%) was added to the binary composition. To some compositions we added 0.5% P267-E4 superfine carbon black. Data on the composition of the binary systems and their combustion characteristics are presented in Table 4. Analyzing these data, we note the following.

Table 3. Melting point of the initial components and compositions E_1 , MC, and E_2

FTDO/DNP	Notation of composition	T_m , °C
0/100	DNP	55
18/82	E_1	38
49/51	MC	62
65/35	E_2	50
100/0	FTDO	112

Compositions 1.1, 1.2, and 1.3 with FTDO/DNP = 18/82 in the range $p = 0.7$ – 4.6 MPa burn without explosion and quenching with a rate ≈ 1 mm/s at $p = 0.7$ MPa and ≈ 4.2 mm/s at $p = 4.6$ MPa. Addition of a metal additive lowers the burning rate by 10–15% relative to the basic composition 1.1. Estimation of the exponent n in the pressure dependence of the burning rate determined at pressures of 2.4 and 4.6 MPa gives values $n \approx 1$ for compositions 1.1 and 1.3 and $n \approx 1.14$ for compositions 1.2.

Temperature profile in the combustion wave was measured using thermocouples. The surface temperature T_s was determined by extinction on a substrate with a flat ribbon Chromel–Alumel thermocouple ≈ 12 μ m thick glued on its surface. In such measurements, the substrate material should have thermophysical properties close to the test substance; therefore ebonite was used [thermal conductivity $\lambda = 0.16$ W/(m · K)]. At $p = 0.5$ and 2.0 MPa, temperatures $T_s = 250$ – 350 °C were recorded.

Table 4. Composition and burning rate of the investigated compositions with varying FTDO/DNP ratio

Notation of composition	(FTDO+DNP) + additives	Burning rate, mm/s at a pressure, MPa		
		≈ 0.7	≈ 2.4	≈ 4.6
1.1	18/82	1.0	2.2	4.2
1.2	94.5% (1.1)* + 0.5% C + 5% Al	0.9	2.0	4.2
1.3	94.5% (1.1) + 0.5% C + 5% AlH ₃	0.9	2.1	4.0
3.1	50/50	(not available)	9.9 / explosion	Explosion
3.2	100% (3.1)** + 2.5% Al	(not available)	8.2	Explosion
3.3	100% (3.1) + 2.5% AlH ₃	(not available)	9.1	25.2
4.1	60/40	(not available)	14 / explosion	Explosion
4.3	100% (4.1) + 3% AlH ₃	(not available)	13.1	Explosion
2.1	65/35	≈ 6.4 / explosion	13.1	Explosion
2.2	94.5% (2.1) + 0.5% C + 5% Al	≈ 6.8 / explosion	13.1	Explosion
2.3	94.5% (2.1) + 0.5% C + 5% AlH ₃	≈ 8	13.1	Explosion

Notes: The simultaneous presence of a value of the burning rate and the word “explosion” in a cell corresponds to the probabilistic nature of the process. This means that some samples normally burned, and others exploded. *Composition 1.2 comprises composition 1.1 with FTDO/DNP = 18/82 and the listed additives. **100% means that the additive was added in excess of 100%.

The temperature in the gas phase was determined using a thermocouple made of tungsten–rhenium wires (95/5 W/Re and 80/20 W/Re) of 50 μm diameter. The thermocouple had an Π -shape with shoulder ≈ 3 mm and was approximately at half the depth of the cup, where it was placed previously, prior to pouring of the sample. For compositions 3.1, the maximum temperature in the gas phase recorded by the thermocouple at $p = 0.7$ and 2.0 MPa, is ≈ 2000 – 2200°C .

Observations of the combustion process in air at 1 atm showed the following. Samples of composition 1.1 usually quenched out without external forcing when the burning surface moved by 5–6 mm into the cup. The burning sample can be quenched by moderate blowing of air (blown out like a candle). When the burning surface had a vertical position, runoff of the liquid surface layer occurs. During combustion of the sample mounted on the substrate, skeleton carbonaceous residues remain after combustion. In the case of an Al additive (composition 1.2), the residues are denser and indicate partial agglomeration of the metal. In the case of AlH₃ additive (composition 1.3), the residues are relatively few and do not appear as agglomerated particles. In both cases (1.2 and 1.3), the metal additive slightly reduces the burning rate.

For the compositions listed in Table 4, experiments were performed to determine the limits of stable combustion at elevated pressure. As seen from

the table, at $p = 2.4$ MPa, the burning rate of compositions 1.1, 1.2, and 1.3 (FTDO/DNP = 8/82) was about 2 mm/s, that of compositions 2.1, 2.2, and 2.3 (FTDO/DNP = 50/50) was about 9 mm/s, and compositions 4.1, 4.3 (FTDO/DNP = 60/40) about 13 mm/s. At the same pressure, for compositions 3.1 and 4.1 explosions were recorded in some cases, and compositions 2.1, 2.2, and 2.3 (FTDO/DNP = 65/35) always exploded.

At $p \approx 4.6$ MPa, compositions with FTDO/DNP = 18/82 burned without explosion and compositions with FTDO/DNP = 50/50, 60/40, and 65/35 exploded (with the exception of composition 3.3 with AlH₃ at a ratio FTDO/DNP = 50/50).

At $p \approx 0.7$ MPa, compositions 1.1, 1.2, and 1.3 (FTDO/DNP = 18/82) burned without explosion; in compositions 2.1 and 2.2 (FTDO/DNP = 65/35), deflagration-to-explosion transition occurred at a probability of $\approx 50\%$, and only composition 2.3 with AlH₃ burned steadily.

Transition to explosion was recorded at burning rates of 8–14 mm/s and above. We can say that the addition of 5% AlH₃ into the binary mixture tends to increase the stability of combustion to a greater extent than the addition of Al.

Samples of compositions 2.1, 2.2, and 2.3 burned steadily in air at atmospheric pressure (in contrast to compositions 1.1). Analysis of the residues of burned

samples 2.2 and 2.3 indicates the formation of a carcass layer on the surface, which is the most dense in the case of composition 2.2 with Al.

Increasing the FTDO content in binary compositions of FTDO/DNP in the series 18/82, 50/50, 60/40, and 65/35 (see Table 4) led to an increase in the burning rate and narrowing of the pressure range of stable combustion. Thus, the mixture E_1 (18/82) burned steadily at $p \leq 4.0$ MPa, and in the case of the mixture E_2 (65/35), deflagration-to-explosion transition occurred starting at $p \approx 0.7$ MPa. Addition of AlH_3 increased the combustion stability.

Thermocouple measurements in combustion of compositions 2.2 and 2.3 at $p \approx 1$ MPa, showed the presence of zones of heat release in the condensed phase at a temperature $\approx 300^\circ C$ and in the gas phase at ≈ 800 and $\approx 1700^\circ C$; the maximum flame temperature was $\approx 3000^\circ C$.

EXPERIMENTAL RESULTS WITH THE COMPOSITIONS BASED ON THE [1FTDO–1DNP] MOLECULAR COMPOUND

Limits of Stable Combustion

In the second phase, we studied compositions (MC) with a fixed ratio FTDO/DNP = 49/51 and various additives. The notation and key formulation features of MC compositions are presented in Table 5. Composition MC-0 is the so-called binary basis [1FTDO–1DNP] with a ratio FTDO/DNP = 49/51, the compositions MC-1, MC-2, MC-3, and MC-4 include AlH_3 , and the composition MC-2, MC-3, and MC-4 include, in addition, energetic substances (AP, ADN, and HMX, respectively). All compositions are hard and brittle and crack during deformation.

The limits of stable combustion were determined at successively increased initial pressure in the combustion vessel starting from 0.5 MPa. At a predetermined pressure level, two samples were typically burned, and the next pair of samples were burned at a higher pressure, in order to determine the critical pressure and burning rate for the given composition. Near the critical conditions, the occurrence of explosion of the tested samples has a probabilistic nature. Explosion could also occur at any stage of combustion of a sample and was accompanied by a typical clip-clopping sound.

Figure 1 shows the pressure dependence of the burning rate of MC-based compositions. The experimental points are connected by straight-line segments. The fact of the explosion of the sample at a certain

Table 5. MC based compositions

Composition	Additive AlH_3 (3.5%)	Energetic additive (15%)
MC-0	—	—
MC-1	+	—
MC-2	+	AP
MC-3	+	ADN
MC-4	+	HMX

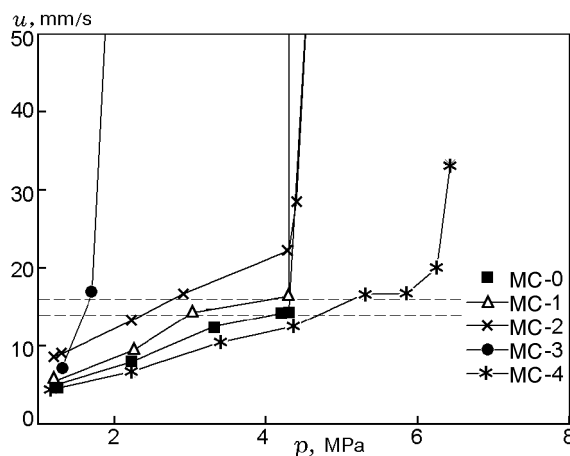


Fig. 1. Limiting burning rate (horizontal dashed lines) above which explosion of the sample occurs. MC type compositions.

pressure is displayed by the assignment of a conditional high burning rate, so that the corresponding point is above the frame of the graph and the line $u(p)$ is almost vertical. As seen in Fig. 1, a condition for the deflagration-to-explosion transition is the attainment of a certain limiting burning rate, rather than the attainment of a certain critical pressure limit. In most cases, explosion occurs at $u = 14$ – 16 mm/s. Because the compositions have individual pressure dependences of the burning rate $u(p)$, the limiting burning rate is achieved at substantially different pressures. For example, for the MC-3 composition, this is ≈ 1.7 MPa, and for MC-4, about 6.3 MPa. It should be noted that the deflagration-to-explosion transition is a complex multi-stage process [25], and special experiments and techniques are required to determine its physical parameters. Therefore, here we restrict ourselves to indicating the critical conditions for the investigated compositions.

Table 6. Typical values of the surface and flame temperatures measured in the combustion in nitrogen at elevated pressure

Composition	p , MPa	T_s , °C	T_f , °C	
			range	average
MC-0	0.5	310±40	2430–2450	2440±10
MC-0	2	?	2500–2570	2535±35
MC-4	0.5	310±40	2420–2520	2470±50
MC-4	2	?	2520–2590	2555±35

Thermocouple Measurements

Experiments to evaluate the temperature parameters of the combustion wave were conducted with samples MC-0 and MC-4 burning in nitrogen at $p = 0.5$ and 2 MPa. The Π -shaped 95/5 W/Re + 80/20 W/Re thermocouple $\varnothing 50 \mu\text{m}$ was placed in the sample in the same manner as in the measurements for binary compositions. Thermocouple records were analyzed using digital signal processing methods involving first filtering for noise suppression and then differentiation in order to identify the points of sharp change in the slope of the curve $T(t)$. One of these points corresponds to the emergence of the thermocouple into the gas phase, i.e., the surface temperature T_s . It should be noted that even after filtering and differentiation, the determination of T_s is not always clear and unambiguous, which is likely due to the fact that the thermocouple shoulder is not parallel to burning surface when entering the gas phase. Another parameter determined by processing the thermocouple signal was the level of the temperature “plateau” in the gas phase. The word “plateau” is in quotes because, in practice, instead of the plateau, there are chaotic temperature fluctuations with an amplitude of about 30–100 K near the mean value. This mean value of the maximum temperature in the gas phase was assumed to be the flame temperature T_f . The characteristic temperatures are presented in Table 6 without any corrections. After the \pm sign the standard deviation calculated for the experiments (number of measurements ≥ 2) is given. The ? sign instead of a numeric value indicates that it was not possible to identify the temperature corresponding to the entry of the thermocouple into the gas phase.

Figure 2 presents thermocouple records for compositions MC-0 and MC-4 at $p = 0.5$ and 2 MPa. The burning rates of the compositions are close: 2.9 and 3 mm/s at 0.5 MPa for MC-0 and 9.5 and 10 mm/s at 2 MPa for MC-4.

From the results of differentiation, it can be noted that in the course of combustion in nitrogen at $p = 0.5$ MPa, the phase and chemical transformations

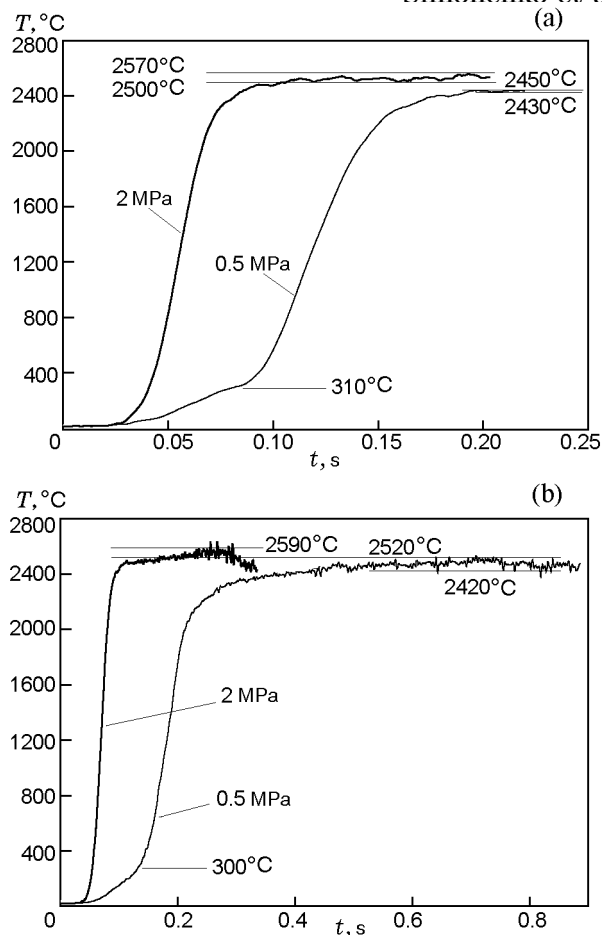


Fig. 2. Record of the thermocouple signal for combustion of MC-0 (a) and MC-4 (b) compositions in nitrogen at $p = 0.5$ and 2 MPa.

in the condensed phase of composition MC-0 occur in the temperature ranges of 40–55 and 170–290°C, and in the case of composition MC-4, which differs from MC-0 by addition of 3.5% AlH_3 and 15% HMX, in the range of 48–240°C. For both compositions MC-0 and MC-4, the entry of the thermocouple into the gas phase occurs at $T_s = 290$ –310°C. For composition MC-0, similar thermocouple experiments were additionally performed in air at a pressure of 0.1 MPa with simultaneous video recording of the combustion process.

Analysis of the data suggests that the flame of MC based compositions at $p = 0.1$ MPa has a temperature of $\approx 1100^\circ\text{C}$, a length of ≈ 3 mm, and is characterized by the presence of a dark zone; the temperature of the secondary flame caused by reaction of the intermediates with the air oxygen is about 1900°C . For combustion in nitrogen at a pressure of 0.5 and 2 MPa, the flame temperature $T_f \approx 2500^\circ\text{C}$. The surface temperatures are, respectively, $T_s \approx 230 \pm 40^\circ\text{C}$ (air; 0.1 MPa) and $T_s \approx 310^\circ\text{C}$ (nitrogen; 0.5 and 2 MPa).

Table 7. Compositions based on MC: critical burning rates and corresponding pressures, at which deflagration-to-explosion transition occurs

Composition	u , mm/s	p , MPa
MC-0	14–16	4.0
MC-1	14–16	4.0
MC-2	16	2.5
MC-3	16	1.5
MC-4	14–16	6.0

CONCLUSIONS

Data were presented on the combustion of: (1) FTDO–DNP mixtures with varying ratio of components (for brevity called binary composition); (2) compositions with the fixed ratio of FTDO/DNP $\approx 49/51$ corresponding to the molecular compound [1FTDO–1DNP] (or MC) with added energetic materials— AlH_3 , AP, ADN, and HMX. Most of the MC type compositions are brittle and have a granular structure at a fracture. In storage under ambient conditions, the behavior of the compositions is individual and depends on the presence of additives. For example, on the surface of an MC-3 sample placed in a cup, ADN crystals were formed in a few (5–10) days. Moreover, the crystals can be found even on the outer surface of the cup.

Analysis of the data on the burning rates and combustion stability revealed a number of regularities.

- The burning rate of binary mixtures increases as the FTDO/DNP ratio changes in the series 18/82, 50/50, 60/40, and 65/35.

- The addition of 3.5% AlH_3 (composition MC-1) leads to a slight increase in the burning rate.

- Addition of one of the energetic substances, AP, ADN, or HMX in an amount of 15% along with 3.5% AlH_3 (compositions MC-2, MC-3, and MC-4, respectively) significantly changes the dependence $u(p)$. Addition of AP and ADN leads to an increase in the burning rate compared with compositions MC-0 and MC-1, and the addition of HMX reduces the burning rate.

- The most important common feature of the behavior of the MC type compositions is that above a certain threshold burning rate, the process becomes unstable and transform to an explosive mode. The limiting burning rate of compositions MC-0, MC-1, MC-2, MC-3, and MC-4 is ≈ 14 – 16 mm/s. The FTDO content in these compositions varies from 49 to 42%. The difference between the dependences $u(p)$ leads to a difference between the pressures at which combustion begins to

show an explosive character (Table 7). Among the compositions MC studied (MC-0, MC-1, MC-2, MC-3, and MC-4 in Table 4), the MC-4–HMX system reaches the critical burning rate at the highest pressure of ≈ 6 MPa.

The results lead to the following conclusions.

1. The burning rate of the FTDO/DNP binary compositions increases when the FTDO concentration increases from 18 to 65%. At a certain burning rate (in the range $u = 8$ – 14 mm/s) there is a transition to an explosive regime. The transition occurs at different pressures because the pressure dependences of the burning rate are individual for compositions with different FTDO/DNP ratio.

2. According to thermocouple measurements in the combustion wave at $p = 0.5$ MPa in nitrogen, the phase transformations and chemical reactions in the condensed phase of the base composition MC-0 (FTDO/DNP = 49/51) occur in the temperature range of 40–55 and 170–290°C, and in the composition MC-4, which differs from MC-0 by the addition of 3.5% AlH_3 and 15% HMX, they occur in the range of 48–240°C. For both compositions (MC-0 and MC-4), the surface temperature is estimated as 290–310°C. The maximum flame temperature at $p = 0.5$ and 2 MPa is in the range of 2500–2600°C.

3. For compositions based on MC (FTDO/DNP $\approx 49/51$ with additives), the critical burning rate is about 16–18 mm/s, above which deflagration-to-explosion transition occurs.

4. Addition of various components to FTDO/DNP based compositions allows control of the burning rate. In particular, its reduction (and the corresponding extension of the pressure range of stable combustion) can be achieved by the addition of HMX.

REFERENCES

1. *Energetic Condensed Systems: Brief Encyclopedic Dictionary*, Ed. by B. P. Zhukov (Yanus-K, Moscow, 2000) [in Russian].
2. V. I. Pepekin, “Trends in Research of Explosives,” *Khim. Fiz.* **29** (12), 8–17 (2010).
3. M. B. Talawar, R. Sivabalan, S. N. zAsthana, and H. Singh, “Novel Ultra-High Energy Materials,” *Fiz. Goreniya Vzryva* **41** (3), 29–45 (2005) [*Combust., Expl., Shock Waves* **41** (3), 264–277 (2005)].
4. V. P. Sinditskii, V. Yu. Egorshv, M. V. Berezin, V. V. Serushkin, Yu. M. Milekhin, S. A. Gusev, and A. A. Matveev, “Combustion Characteristics and Mechanism of the High-Energy Caged Nitramine Hexanitrohexaazaisowurtzitane,” *Zh. Khim. Fiz.* **22** (7), 64–69 (2003).

5. V. P. Sinditskii, V. Yu. Egorshv, and M. V. Berezin, "Investigation of Combustion Energy-Cyclic Nitramines," *Zh. Khim. Fiz.* **22** (4), 53–60 (2003).
6. A. M. Churakov, S. L. Ioffe, and V. A. Tartakovsky, "Synthesis of [1,2,5]oxadiazolo[3,4-e][1,2,3,4]tetrazine 4,6-di-N-oxide," *Mendeleev Commun.* **5** (6), 227–228 (1995).
7. V. P. Zelenov, A. A. Lobanova, N. I. Lyukshenko, S. V. Sysolyatin, and A. I. Kalashnikov, "Behavior of [1,2,5]oxadiazolo[3,4-e][1,2,3,4] tetrazine-4,6-di-N-oxide in Various Environments," *Izv. Akad. Nauk, Ser. Khim.*, No. 7, 1358–1362 (2008).
8. V. G. Kiselev, N. P. Gritsan, V. E. Zarko, P. I. Kalmykov, and V. A. Shandakov, "Multilevel Quantum Chemical Calculation of the Enthalpy of Formation [1,2,5]oxadiazolo[3,4-e][1,2,3,4] tetrazine-4,6-di-N-dioxide," *Fiz. Goreniya Vzryva* **43** (5), 77–81 (2007) [*Combust., Expl., Shock Waves* **43** (5), 562–566 (2007)].
9. V. I. Pepekin, Yu. N. Matushin, and T. V. Gubina, "Enthalpy of Formation and Explosive Properties of Furazanotetrazine Dioxide," *Khim. Fiz.* **30** (2), 42–45 (2011).
10. V. A. Teselkin, "Mechanical Sensitivity of Furazano-1,2,3,4-tetrazine-1,3-dioxide," *Fiz. Goreniya Vzryva* **45** (5), 140–142 (2009) [*Combust., Expl., Shock Waves* **45** (5), 632–633 (2009)].
11. P. I. Kalmykov, Yu. N. Burtsev, N. P. Kuznetsova, and V. V. Konstantinov, "Phase State and Structure Formation of Eutectic Alloys Based on DF-2," in *III All-Russian Conf. Energetic Condensed Systems, Chernogolovka, 2006*, pp. 64–66.
12. D. B. Lempert, G. N. Nechiporenko, and S. I. Soglasnova, "Dependence of the Specific Impulse of Rocket Propellant Compositions Containing Oxidizers Based on C, N, and O Atoms on the Enthalpy of Formation of the Elemental Composition of the Oxidizer," *Khim. Fiz.* **23** (5), 75–81 (2004).
13. V. P. Sinditskii, A. V. Burzhava, V. Yu. Yegorshev, A. B. Sheremetev, and V. P. Zelenov, "Combustion of Furazanotetrazine Dioxide," *Fiz. Goreniya Vzryva* **49** (1), 134–137 (2013) [*Combust., Expl., Shock Waves* **49** (1), 117–120 (2013)].
14. U. R. Nair, R. Sivabalan, G. M. Gore, M. Geetha, S. N. Asthana, and H. Singh, "Hexanitrohexaazaisowurtzitane (CL-20) and CL-20-based Formulations (Review)," *Fiz. Goreniya Vzryva* **41** (2), 3–16 (2005) [*Combust., Expl., Shock Waves* **41** (2), 121–132 (2005)].
15. M. B. Talawar, R. Sivabalan, M. Anniyappan, M. B. Gore, S. N. Asthana, B. R. Gandhi, "Emerging Trends in Advanced High-Energy Materials," *Fiz. Goreniya Vzryva* **43** (1), 72–85 (2007) [*Combust., Expl., Shock Waves* **43** (1), 62–72 (2007)].
16. P. I. Kalmykov, A. A. Sidel'nikov, A. I. Ancharov, I. V. Koptyug, V. E. Zarko, and T. P. Ryabchikova, "Investigation of the Crystallization and Phase Structure of FTDO–DNP Binary Systems," in *Abstracts IV All-Russian Conf. Energetic Condensed Systems, Chernogolovka, 2008*, pp. 26–27.
17. P. I. Kalmykov, V. E. Zarko, V. N. Simonenko, G. V. Romanenko, K. A. Sidorov, R. V. Rafikov, V. V. Erofeev, and A. V. Pozdnyakov, "Relationship between the Phase Structure and Combustion Behavior of FTDO–DNP Binary Systems," in *V All-Russian Conf. Energetic Condensed Systems, Chernogolovka, 2010*, pp. 134–136.
18. P. I. Kalmykov, V. E. Zarko, V. N. Simonenko, N. P. Vdovina, O. A. Troshina, and K. A. Sidorov, "Relationship between the Physicochemical Transformations of Furazanotetrazine Dioxide (FTDO) and the Combustion Behavior of Condensed Systems Based on It," in *XIV Symposium on Combustion and Explosion: Combustion and Kinetics, Chernogolovka, 2008*, p. 79.
19. P. I. Kalmykov, V. E. Zarko, A. A. Sidelnikov, I. V. Koptyug, A. I. Ancharov, and K. A. Sidorov, "Crystal and Phase Structures of 5,6-(3¹,4¹-furazano)-1,2,3,4-tetrazine-1,3-dioxide-2,4-dinitro-2,4-diazapentane Binary Systems," *Zh. Prikl. Khim.* **84** (2), 252–259 (2011).
20. P. I. Kalmykov, Yu. N. Burtsev, N. P. Kuznetsova, I. A. Merzhanov, G. V. Romanenko, K. A. Sidorov, E. V. Artemova, V. V. Zakharov, and N. V. Chukanov, "Crystallization from the Melt and Phase Analysis of the [FTDO–DNP] Molecular Compound," in *VI All-Russian Conf. Energetic Condensed Systems, Chernogolovka, 2012*, pp. 54–58.
21. V. E. Zarko, A. A. Kvasov, A. I. Ancharov, K. E. Kuper, A. B. Kiskin, V. N. Simonenko, "X-ray Diffraction and Microscopy Studies of the Structure of Molecular Compound FTDO–DNAP," in *40th Int. Conf. of ICT Energetic Materials. Characterization. Modeling and Validation, Karlsruhe, Germany, 2009*, pp. 98–1–98–10.
22. A. P. Denysiuk, Yu. G. Shepelev, S. V. Yudaev, and I. V. Kalashnikov, "Combustion of Systems Containing Linear Nitramines," *Fiz. Goreniya Vzryva* **41** (2), 98–107 (2005) [*Combust., Expl., Shock Waves* **41** (2), 206–214 (2005)].
23. A. G. Gorst, *Gunpowder and Explosives* (Gosizdatoboronprom, Moscow, 1957) [in Russian].
24. K. K. Andreev and A. F. Belyaev, *Theory of Explosives* (Gosoborongiz, Moscow 1960) [in Russian].
25. A. F. Belyaev, V. K. Bobolev, A. I. Korotkov, A. A. Sulimov, and S. V. Chuiko, *Deflagration-to-Explosion Transition in Condensed Systems* (Nauka, Moscow, 1973) [in Russian].
26. V. E. Zarko, V. N. Simonenko, P. I. Kalmykov, A. A. Kvasov, E. N. Chesnokov, and K. E. Kuper, "Laser Initiation and Crystallized Mixtures of Furazanotetrazine Dioxide Dinitrodiazapentane," *Fiz. Goreniya Vzryva* **45** (6), 131–134 (2009) [*Combust., Expl., Shock Waves* **45** (6), 752–755 (2009)].